SUPPLEMENTAL MATERIAL

1. Experimental set up and procedure

1.1 Starting material

Andesitic lava, without any apparent alteration, was sampled from the Whangaehu valley, Ruapehu volcano, New Zealand (NZTM 1823141 5648537). $^{40}Ar/^{39}Ar$ dating reveals an age of < 5 kyr for the lava (Conway et al., 2016; Townsend et al., 2017). Major element data confirms the andesitic composition of the lava, while the loss on ignition (LOI) indicates that the lava sample was unaltered (Table DR1).

Table DR1: Normalised whole-rock major element data for the andesite sample used in the experiments, with the original LOI and total.

SiO_2 (%)	Al_2O_3 (%)	TiO_2 (%)	MnO (%)	Fe_2O_3 (%)	MgO (%)	CaO (%)	Na_2O (%)	K_2O (%)	P_2O_5 (%)	SO_3 (%)	Sr (ppm)	Ba (ppm)	LOI	Original Total
59.66	16.92	0.67	0.11	6.69	4.12	6.50	3.48	1.60	0.15	0.02	289	371	-0.15	99.74

1.2 Experimental setup

The experiments were carried out at the Physical Volcanology Laboratory, University of Würzburg, Germany. A calorimeter was set up consisting of an insulated, stainless steel tank containing ~ 3 liters of distilled, room temperature water. The tank was positioned on a balance and contained eight K-type thermocouples, calibrated with a precision of 0.3 K and a response rate of 4 Hz, placed symmetrically below the water level. A stirrer forced convection in the water to prevent stratification and to homogenize the water temperature.

For the molten andesite-ice experiments, the ice was made from a mixture of crushed ice and 0 °C water, which was frozen in a silicone mould. In order for deformation to occur, a squeeze apparatus was designed and manufactured at the University of Otago. The apparatus consisted of a set of tongs with paddles that were brought together when the opposing arms were squeezed. The paddles and lower sections of the arms were made of wood, which has a low thermal conductivity. One paddle was frozen onto the ice block with a wooden dowel to secure the ice to the wood. Prior to each experiment, the remaining paddle was soaked in water. Strain gauges (RS Pro foil) and a straight beam load cell (HT Sensor TAL220) were fixed to the arms of the tongs to measure the pressure applied during squeezing.

The rim of the calorimeter was manually tapped before the beginning of each experiment to produce a mass spike, and a blinking LED light was used to indicate the start of logging from the load cells. Both of these indicators were caught on video to later synchronise the data loggers that recorded the water temperature and mass with the data logger for the load cells. All experiments were carried out at room temperature, and the ambient pressure was measured.

1.3 Thermal properties

Simple calorimetric experiments were first performed to quantify the specific heat capacity (C_L), thermal diffusivity (K) and thermal conductivity (k) of the andesite. The molten andesite was dropped into the calorimeter and the temperature of the water was measured every 0.25 seconds until there was no further increase, and the water and melt (solidified to glass) were assumed to have attained thermal equilibrium (Fig. DR1A). The energy transfer determinations and subsequent calculations of the thermal properties follow the procedure given by Oddsson et al. (2016). The measured variables

and calculated thermal properties are shown in Table DR2. The energy used to heat the water (E_w) was found by

$$E_w = m_w c_w \Delta T_w \qquad \text{(equation 1)}$$

where m_w is the mass of the water (kg), c_w is the specific heat capacity of water (4187 J kg^{-1} K^{-1}) and ΔT_w is the overall temperature change of the water due to heating by the andesite. Where no visible steam was produced, heat transfer is assumed to have taken place within a closed system (Oddsson et al., 2016). The energy transferred to heat the water can, therefore, be assumed as equal to the initial heat content of the melt (E_m):

$$E_w = E_m \qquad \text{(equation 2)}$$

Thus, this andesite's specific heat capacity (c_L) can be calculated by rearranging equation 1 such that:

$$c_L = \frac{E_m}{m_L \, \Delta T} \qquad \text{(equation 3)}$$

where m_L is the mass of the melt (kg) and ΔT is the overall temperature change of the andesite during cooling in the water. The initial temperature of the melt was $\sim$ 1250 °C. The latent heat of crystallisation was not considered here, or in any further calculations, because only glass was formed by the rapid cooling of the melt (Gudmundsson et al., 1997; Oddsson et al., 2016). It is assumed that all of the energy transferred was in the form of heat. A time series of E_m was determined in order to calculate the time-progressive heat flux (q) by:

$$q = \frac{1}{A}\left(\frac{dE}{dt}\right) \qquad \text{(equation 4)}$$

where A is the surface area of the melt (m^2), and t is time (s). The surface area of the melt was measured on ImageJ using photographs of the solidified andesite samples. In some cases, the sample had broken into pieces and an estimate of the area in contact with the water (or ice for the deformation experiments) was made. The cumulative heat transfer (Q) was then calculated to determine the thermal diffusivity (κ) of the Ruapehu andesite, following (Oddsson et al., 2016), thus:

$$\kappa = \frac{\pi}{4(\rho c_L \Delta T)^2}\alpha^2 \qquad \text{(equation 5)}$$

where ρ is the density of the melt, determined from the wet and dry masses of each sample (Houghton and Wilson, 1989), and α is the initial gradient of Q when plotted against $\sqrt{t}$ (Fig. DR1B). Finally, the thermal conductivity (k), could be found as a simple function of the heat capacity and thermal diffusivity:

$$k = \rho c_L \kappa \qquad \text{(equation 6)}$$

Table DR2: Measured variables and calculated thermal properties for Ruapehu andesite samples, determined by calorimetry. During runs 3-5, the melt was poured from the crucible into the calorimeter. The high viscosity of the melt meant that the lava spent up to 30 seconds cooling in air to an unknown temperature before reaching the calorimeter. For run 6, the melt was scooped from the crucible and placed directly into the calorimeter. No visible steam was produced during this run. The results from run 6 are therefore deemed to be most reliable and are used as the thermal properties of Ruapehu andesite in subsequent calculations.

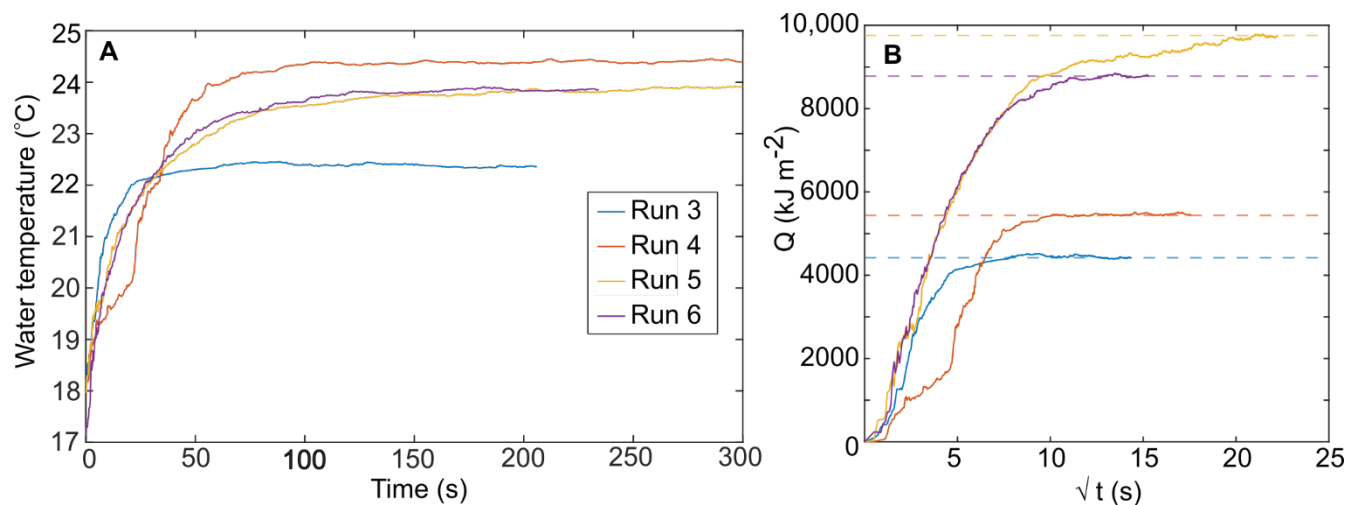| Experimental run	Andesite mass (kg) $\pm 10^{-6}$	Andesite surface area (m^2)	Andesite density (kg m^{-3})	Water mass (kg) $\pm 10^{-4}$	Specific heat capacity (J kg^{-1} K^{-1})	Thermal diffusivity (m^2 s^{-1})	Thermal conductivity (W m^{-1} K^{-1})
3	6.343×10^{-2}	120×10^{-4}	2220 ± 2	3.001	680 ± 49	$1.9 \pm 0.2 \times 10^{-7}$	0.3 ± 0.04
4	7.605×10^{-2}	144×10^{-4}	2450 ± 2	3.002	841 ± 22	$1.8 \pm 0.1 \times 10^{-8}$	0.04 ± 0.002
5	6.789×10^{-2}	80×10^{-4}	2150 ± 1	3.005	933 ± 32	$1.9 \pm 0.1 \times 10^{-7}$	0.4 ± 0.03
6	7.855×10^{-2}	96×10^{-4}	2170 ± 0.3	3.000	878 ± 44	$2.1 \pm 0.2 \times 10^{-7}$	0.4 ± 0.04

Figure DR1: A: Change in calorimeter water temperature following immersion of andesite sample. B: Cumulative heat transfer against the square root of time. The initial gradient was used for calculating thermal diffusivity. Dashed lines show the maximum possible heat transfer for each sample.

1.4 Molten andesite-ice deformation experiments

During the dynamic andesite-ice interaction experiments, the melt was squeezed between the ice block and a wet wooden paddle. The melt was extracted from the crucible, about a meter away, and transferred immediately to the squeeze apparatus. Measured and calculated results concerning meltwater production, thermal energy, and heat flux are shown in Table DR3. The mass of the andesite sample was measured after the experiment, so there is no error associated with mass lost to the crucible. Meltwater was collected in the calorimeter so that the mass (m_m) was recorded (Fig. DR2A). The ice block was also weighed before and after each experiment to provide a further measure on the overall volume of meltwater produced by the interaction. Runs 14-16 were carried out using a small bowl containing 400-600 ml of water, replacing the tank containing 3 liters of water (the mass of calorimeter water used for each run is shown in Table DR3). The smaller calorimeter could be placed on a balance of higher sensitivity so that small changes in the mass of the accumulating meltwater could be measured with greater precision. Some steam was produced during these runs, however. One K-type thermocouple was placed in the water at the base of the bowl. In this set-up, water mass and temperature data were not recorded to a data logger, but read directly from the instruments, which were positioned in view of the cameras. Data were later extracted from the frames. The temperature of the meltwater (T_m) for all andesite-ice deformation runs was determined by:

$$T_m = \frac{T_1 m_1 - T_0 m_0}{m_m} \qquad \text{(equation 7)}$$

where T_1 and m_1 are the temperature and mass of the water, respectively, in the calorimeter at the end of the experiment, and 0 denotes the temperature and mass at the start of the experiment. The rate of thermal energy transfer was then calculated by:

$$\frac{dE}{dt} = \frac{dm}{dt}(c_i \Delta T_i + L_i + c_w \Delta T_m) \qquad \text{(equation 8)}$$

where dm/dt is the meltwater production rate, c_i is the specific heat capacity of ice (2108 J kg^{-1} K^{-1}), ΔT_i is the temperature difference between the ice at the start of the experiment and its melting point, and L_i is the specific latent heat of melting of ice (334 kJ kg^{-1}) (Oddsson et al., 2016). The heat flux throughout the experiment was then calculated by equation 4. In addition to the time-series, the overall meltwater production and heat flux were also calculated.

The molten andesite squeezed well against the ice until it had melted a cavity and was no longer being pushed or deformed by the opposing paddle. At this point, the paddle was retracted and the melt dropped into the calorimeter, where its remaining thermal energy caused a rapid temperature rise in the water. The thermal energy transferred to the water could be calculated using equation 1, and again assumed to equal the thermal energy released by the melt after deformation against ice (E_{mf}). Therefore, the temperature to which the melt cooled while being deformed against the ice (T_{lava}) could be calculated by rearranging equation 3:

$$T_{lava} = \frac{E_{mf}}{m_L c_L} + T_{amb} \qquad \text{(equation 9)}$$

where T_{amb} is ambient temperature, and where ΔT in equation 3 is equal to $T_{lava} - T_{amb}$. This allows the overall temperature loss of the melt from contact with ice to be estimated. Assuming an initial melt temperature of 1250 °C, the thermal energy extracted from the melt during the experiment (E_{mi}) could be determined. In addition, the thermal energy used to melt the ice (E_i) was calculated by the same energy equation:

$$E_i = m_i(c_i \Delta T_i + L_i) \qquad \text{(equation 10)}$$

where m_i is the mass of ice melted, measured as the mass of meltwater collected (kg). The efficiency of heat transferred (f_e) from the andesite to melt the ice, was determined by:

$$f_e = \frac{E_i}{E_{mi}}$$ (equation 11)

Note that this equation only considers the energy used in melting the ice and does not reflect heat transferred from the melt to its surroundings, for example to heat the meltwater produced or heat loss to the air (Gudmundsson et al., 2004).

Figure DR2B shows the cumulative heat transfer from the andesite melt to the ice during squeezing. The horizontal lines mark the maximum theoretical limit of heat that could be transferred from the andesite to the ice over the interface area. The cumulative curves generally fall short of the limit, which we infer is due to heat transferred to the ice to warm it, but not melt it. The temperature of the ice was not measured during the experiments, but it is probable that heat would have been transferred to more ice than was melted. Calculations of the total heat energy required to raise the ice temperature to 0 °C without melting it give energy values between 2×10^6 and 18×10^6 Jm^{-2}, indicating that the ice is a large heat sink and accounting for the energy gap between most of the curves and their maximum limits. Runs 13 and 14 are anomalous due to error associated with the calculated temperature of the andesite after deformation with ice. Run 13 had a very short duration due to the andesite melting through the bottom of the ice and slipping out of the squeeze apparatus after only a few seconds. The temperature of the melt was still high, meaning ΔT_m and therefore the total theoretical heat transfer is low. For Run 14, ΔT_m is high because the calculated temperature of the andesite after deformation against ice is probably an underestimate due to a delay in the rise of the water temperature in the calorimeter after the lava was dropped into it because the water was not stirred initially.

1.5 Limitations of the apparatus

These experiments were a first attempt at investigating the dynamic interaction between andesite lava and ice. We present a qualitative relationship between applied pressure and meltwater production and heat transfer. There is scope for refinement of this experimental procedure and opportunity to quantify the relationship between moving lava and ice on meltwater production. An additional set of experiments is required that addresses some of the difficulties and uncertainties we faced, including instrument failure.

Issues with data-output from the pressure sensors, particularly the RS Pro foil strain gauge, meant we present the applied force during the deformation experiments in arbitrary units. For some runs, no data was recorded from the pressure sensors. The straight beam load cell worked more consistently and is recommended for further experiments. It would also be useful devise a way to track the change in surface area during deformation as this could provide a more detailed record of meltwater production with increased deformation.

A balance with a 1 g measurement error was used for runs 10-13 meaning small increases in meltwater mass were not recorded or recognition of a small change in mass was delayed. The overall meltwater production rates and heat fluxes were determined for these runs, however, as presented in Table DR3. A more sensitive balance with a 0.01 g measurement error was used for runs 14-16, which was more responsive to the increases in meltwater and allowed meltwater production and heat transfer to be calculated continuously throughout the experiment. A smaller calorimeter containing a smaller water volume was used with this balance, however, meaning that some steam was produced and thermal energy released into the atmosphere.

There are large errors associated with the temperature of the meltwater for all deformation runs because the volume of meltwater added to the calorimeter was small compared with the initial volume of water. It would be preferable to measure the temperature of the meltwater directly before it reaches

the calorimeter. In addition, it would be helpful to measure the temperature of the ice during the experiments to record the heat transfer that must occur that causes the ice to warm, but not melt.

Table DR3: a) Measured values during the andesite melt-ice deformation experiments (top); b) Overall results of each andesite melt-ice deformation experiment, calculated as explained in text (bottom). The water temperature was not measured for runs 8 and 9 and so the melt temperature and heat flux (q) could not be determined.

Experimental run	Temperature of ice (° C)	Mass loss of ice (kg)	Total mass of meltwater (kg)	Mass of melt (kg)	Melt-ice interface surface area (m²)	Initial mass of water (kg)	Initial thermal energy (kJ)
8	-28	-	0.089	0.07969	33×10^{-4}	-	107
9	-28	-	0.113	0.09035	28×10^{-4}	-	121
10	-28	0.039	0.028	0.10068	42×10^{-4}	3.002	135
11	-8	0.011	0.013	0.02404	13×10^{-4}	3.033	32
12	-28	0.023	0.022	0.05884	23×10^{-4}	3.009	79
13	-28	0.015	0.012	0.06622	38×10^{-4}	3.053	89
14	-5	0.047	0.036	0.06495	35×10^{-4}	0.415	87
15	-28	0.053	0.047	0.09154	55×10^{-4}	0.604	122
16	-28	0.044	0.037	0.1033	48×10^{-4}	0.603	138

Experiment	Overall meltwater production rate (kg/s)	Average meltwater temperature (°C)	Final Temperature of melt (°C)	Em (J)	Ei (J)	fe	q (kWm⁻²)
10	$1.80 \pm 0.09 \times 10^{-3}$	40 ± 18	940 ± 49	$2.74 \pm 0.45 \times 10^{4}$	$1.10 \pm 0.06 \times 10^{4}$	0.40 ± 0.07	243 ± 36
11	$0.68 \pm 0.07 \times 10^{-3}$	6 ± 91[‡]	890 ± 168	$0.76 \pm 0.36 \times 10^{4}$	$0.45 \pm 0.05 \times 10^{4}$	0.60 ± 0.30	194 ± 200
12	$1.00 \pm 0.07 \times 10^{-3}$	40 ± 46	985 ± 74	$1.37 \pm 0.39 \times 10^{4}$	$0.87 \pm 0.06 \times 10^{4}$	0.63 ± 0.18	250 ± 86
13	$2.67 \pm 0.30 \times 10^{-3}$	35 ± 64	1164 ± 68	$0.50 \pm 0.39 \times 10^{4}$	$0.47 \pm 0.06 \times 10^{4}$	0.95 ± 0.77	385 ± 196[#]
14	$1.81 \times 10^{-3} \pm 7 \times 10^{-7}$	19 ± 17	641 ± 45*	$3.47 \pm 0.31 \times 10^{4}$	$1.25 \pm 0.01 \times 10^{4}$	0.36 ± 0.03	222 ± 36
15	$2.23 \pm 0.07 \times 10^{-3}$	18 ± 19	865 ± 53	$3.10 \pm 0.45 \times 10^{4}$	$1.84 \pm 0.06 \times 10^{4}$	0.60 ± 0.09	200 ± 35
16	$1.69 \pm 0.06 \times 10^{-3}$	31 ± 23	881 ± 51	$3.34 \pm 0.49 \times 10^{4}$	$1.46 \pm 0.06 \times 10^{4}$	0.44 ± 0.07	186 ± 35

[‡]The andesite melt of run 11 had cooled in the air for several more seconds before interaction with ice, accounting for a cooler meltwater temperature.
[#]Run 13 lasted only 5 s before the andesite melted through the bottom of ice and dropped into the calorimeter. The total heat flux is, therefore, apparently higher because it represents the very initial contact.
*The final temperature of the melt after run 14 is probably an underestimate because there was a delayed rise in water temperature after the melt sample was dropped into the calorimeter due to a delay before stirring commenced.
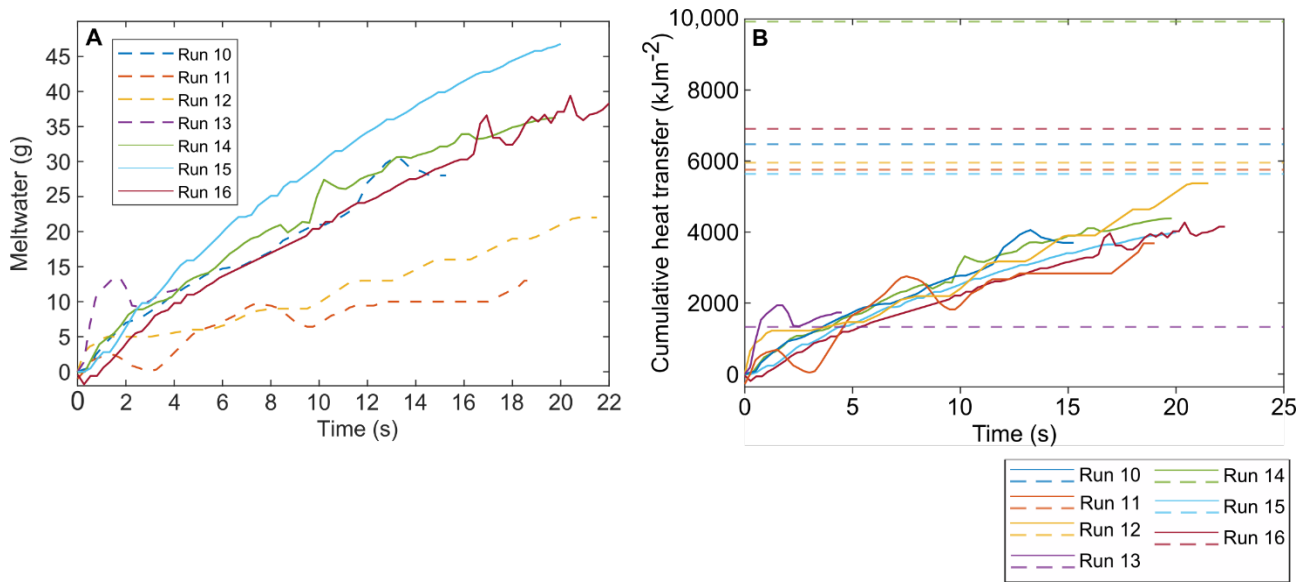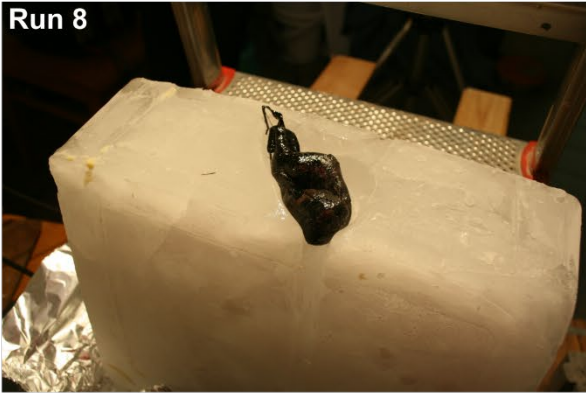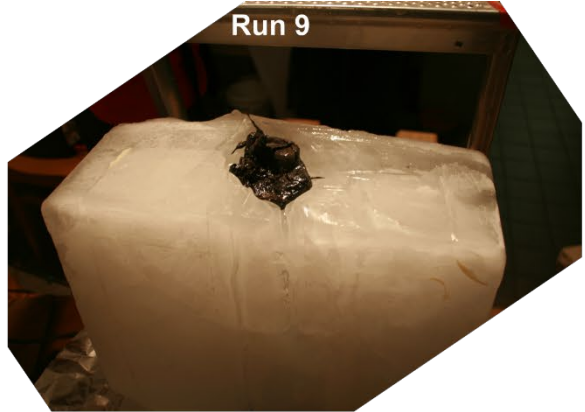
Figure DR2: A: Meltwater accumulation during Runs 10-16. B: Cumulative heat transfer from andesite melt to ice during deformation experiments. Dashed lines show maximum possible heat transferred over ice-melt interface for each sample.

Run 8

Run 9

Run 10

Run 12

Run 14

6 cm

Run 15

Run 16

Run 16

Figure DR3: Photographs of quenched andesite samples after selected experimental runs and an example of the eroded ice block. For runs 8 and 9, the andesite sample was placed on top of the ice block at rest (Run 8) or pushed into the ice (Run 9). The photos show the andesite sitting in the cavity it formed in the ice, with the meltwater channels that were carved into the ice block.

2. References

Conway, C.E., Leonard, G.S., Townsend, D.B., Calvert, A.T., Wilson, C.J.N., Gamble, J.A., and Eaves, S.R., 2016, A high-resolution 40Ar/39Ar lava chronology and edifice construction history for Ruapehu volcano, New Zealand: Journal of Volcanology and Geothermal Research, v. 327, p. 152–179, doi:10.1016/j.jvolgeores.2016.07.006.

Gudmundsson, M.T., Sigmundsson, F., and Björnsson, H., 1997, Ice-volcano interaction of the 1996 Gjalp subglacial eruption, Vatnajokull, Iceland: Nature, v. 389, p. 954–957, doi:10.1038/40122.

Gudmundsson, M.T., Sigmundsson, F., Björnsson, H., and Högnadóttir, T., 2004, The 1996 eruption at Gjálp, Vatnajökull ice cap, Iceland: Efficiency of heat transfer, ice deformation and subglacial water pressure: Bulletin of Volcanology, v. 66, p. 46–65, doi:10.1007/s00445-003-0295-9.

Houghton, B.F., and Wilson, C.J.N., 1989, A vesicularity index for pyroclastic deposits: Bulletin of Volcanology, v. 51, p. 451–462, doi:10.1007/BF01078811.

Oddsson, B., Gudmundsson, M.T., Sonder, I., Zimanowski, B., and Schmid, A., 2016, Experimental studies of heat transfer at the dynamic magma ice/water interface: Application to subglacially emplaced lava: Journal of Geophysical Research: Solid Earth, v. 121, p. 3261–3277.

Townsend, D.B., Leonard, G.S., Conway, C.E., Eaves, S.R., and Wilson, C.J.N., 2017, Geology of the Tongariro National Park Area: GNS Science Geological Map 4, p. 1 sheet + 109 pp.